



# Highly efficient CO removal by active cuprous-based ternary deep eutectic solvents [HDEEA][Cl] + CuCl + EG

Guokai Cui, Kang Jiang, Huayan Liu, Ying Zhou, Zekai Zhang, Ruina Zhang, Hanfeng Lu\*

*Institute of Catalytic Interaction Engineering, College of Chemical Engineering, Zhejiang University of Technology, 18 Chaowang Road, Hangzhou 310014, China*

## ARTICLE INFO

### Keywords:

Deep eutectic solvent  
Cuprous  
CO  
Removal  
Anion

## ABSTRACT

Carbon monoxide (CO) is a kind of impurity gas in hydrogen (H<sub>2</sub>), resulting to catalyst poisoning in proton-exchange-membrane fuel cells (PEMFCs). On the other hand, CO is harmful to human health due to its colorlessness, odorlessness and high toxicity. In this contribution, a series of active cuprous-based ternary deep eutectic solvents (DESSs) with 2-diethylaminoethanol chloride ([HDEEA][Cl]) plus cuprous chloride (CuCl) plus ethylene glycol (EG) at different molar ratios (1:1:4, 1:1:2 and 1:1:1) were designed and prepared. Physical properties such as density and viscosity of these DESSs were measured at different temperatures. CO capture by these DESSs were investigated at different concentrations of CO and different temperatures. It was found that the capture capacities of 0.203 and 0.564 mol CO per mole DES could be reached by [HDEEA][Cl] + CuCl + EG with  $n_{[HDEEA][Cl]}:n_{CuCl}:n_{EG} = 1:1:4$  at 293.2 K and 1 bar or 5 bar, respectively. FT-IR method was used to investigate the mechanism of CO removal. These results suggested that the presence of Cu(I) is crucial for efficient capture of CO by these ternary DESSs while –OH groups and EG could release the activity of Cu(I). Furthermore, the thermodynamic properties such as the Gibbs free energy change ( $\Delta G$ ), enthalpy change ( $\Delta H$ ), and entropy change ( $\Delta S$ ) for CO capture by [HDEEA][Cl] + CuCl + EG (1:1:4) were obtained, and  $\Delta H$  was the main driving force for CO capture.

## 1. Introduction

Carbon monoxide (CO) is a kind of impurity gas in hydrogen (H<sub>2</sub>), resulting in the catalyst poisoning in proton-exchange-membrane fuel cells (PEMFCs) [1]. On the other hand, CO is harmful to human health due to its colorlessness, odorlessness and high toxicity. Therefore, CO capture has received increasing attention with the development of industry, especially low-concentration CO removal. Numerous purification technologies have been employed for CO removal, including Cu(I)-based method [2], pressure swing adsorption (PSA) method [3] and supported liquid membranes (SLMs) method [4]. Among these technologies, a kind of aromatic bimetallic cuprous salt solution, usually CuAlCl<sub>4</sub> dissolved in toluene, was developed in the 1970 s and named COSORB process for CO capture, resulting in the stability of complex but the loss of solvent [5]. Thus, exploring environmentally friendly technologies for efficient CO removal is important.

In recent decades, ionic liquids (ILs) as a kind of promising absorbent for gas capture are well-known due to their high thermal stability, negligible vapor pressure, wide liquid temperature range, and tunable

structures [6–10]. Several kinds of ILs, especially anion- or cation-functionalized ILs were developed for gas capture, such as SO<sub>2</sub>, [11–14] CO<sub>2</sub>, [15–18] H<sub>2</sub>S, [19–20] NO<sub>x</sub> [21–22] and NH<sub>3</sub> [23–25]. For the purpose of CO removal, Laurenczy *et al.* reported the solubility of CO in ILs for the first time, and the solubility increased according to [Bmim][BF<sub>4</sub>] < [Bmim][PF<sub>6</sub>] < [Bmim][SbF<sub>6</sub>] < [Bmim][CF<sub>3</sub>COO] < [Bmim][Tf<sub>2</sub>N]. [26] Tao *et al.* reported that up to 0.046 mol CO per mole IL could be obtained by [P<sub>4448</sub>][Pen] at 298.2 K and 1 bar [27]. Considering that CO could be captured by copper(I) based absorbents, CO capacities of 0.020 and 0.078 mol CO per mole IL by [hmim][CuCl<sub>2</sub>] and [TEA][CuCl<sub>2</sub>] at 303.2 K and 1 bar were reported by Urriaga *et al.* [28] and Hu *et al.*, [29] respectively. More recently, an IL [EimH][CuCl<sub>2</sub>] was reported to absorb 0.118 mol CO per mole IL at 303.2 K and 1 bar [30]. Although these cuprous-based ILs were developed and showed improved solubilities for CO removal compared with conventional ILs, the viscosity of ILs, especially protic ILs, is usually very high, which limits the activity of Cu(I) on CO capture [31].

As a kind of ionic liquid analogues, deep eutectic solvents (DESSs) are particularly interesting due to their fine-tuned physical-chemical

\* Corresponding author.

E-mail address: [luhf@zjut.edu.cn](mailto:luhf@zjut.edu.cn) (H. Lu).

<https://doi.org/10.1016/j.seppur.2021.118985>

Received 25 February 2021; Received in revised form 29 April 2021; Accepted 15 May 2021

Available online 19 May 2021

1383-5866/© 2021 Elsevier B.V. All rights reserved.

properties through choosing suitable hydrogen bond acceptors (HBAs) and hydrogen bond donors (HBDs). [32–36] First example of DES was reported by Abbott *et al.*, and the DES can be easily prepared through mixing cholinium chloride (ChCl) as a HBA with urea as a HBD [37]. In recent years, kinds of DESs were designed and prepared for the capture of SO<sub>2</sub>, [38–39] CO<sub>2</sub>, [40–41] NO<sub>x</sub> [42–43] and NH<sub>3</sub>. [44–46] For instance, Han *et al.* [47] reported the first SO<sub>2</sub> capture by [Ch][Cl]-based DESs with glycerol (Gly) as the HBD. Huang *et al.* showed the thermodynamic and molecular insights into the capture of H<sub>2</sub>S, CO<sub>2</sub>, and CH<sub>4</sub> by [Ch][Cl] + urea mixtures. [48] Choi *et al.* reported CO<sub>2</sub> capture by monoethanolamine hydrochloride plus ethylenediamine in molar ratios from 1:1 to 1:4. [49] Cui *et al.* developed a kind of tertiary amine-containing [PPZ][Br] + Gly DESs which exhibited that up to 4.28 mol SO<sub>2</sub> per mole [PPZ][Br] + Gly (1:6) could be captured at 293.2 K and 1 bar. [50] Deng *et al.* showed that [NH<sub>4</sub>][SCN]-based DES could efficiently absorb NH<sub>3</sub> [51]. The above investigations reveal whether CO can be removed by cuprous-based DESs. Very recently, Tao *et al.* [52] reported a kind of ternary DES [BimH][Cl] + CuCl + ZnCl<sub>2</sub> (1:1:1) which exhibited high CO capture capacity up to 0.075 mol CO per mole IL under 1 bar and 353.2 K. However, this DES containing two metals has very high viscosity (about 6000 mPa s at 313.2 K). Thus, DESs with low viscosity and high capacity are highly desired.

Herein, we designed a series of low viscosity ternary DESs with 2-diethylaminoethanol hydrochloride ([HDEEA][Cl]) and cuprous chloride (CuCl) as two HBAs and ethylene glycol (EG) as a HBD (Scheme 1). Physical properties, such as density and viscosity, of these DESs were determined. The performances of CO capture by these DESs with different molar ratio of [HDEEA][Cl]:CuCl:EG (1:1:1, 1:1:2, and 1:1:4) were investigated at different partial pressures of CO and temperatures. Molar capacities of 0.203 and 0.564 mol CO per mole DES could be obtained by [HDEEA][Cl] + CuCl + EG (1:1:4) at 293.2 K and 1 bar or 5 bar CO partial pressure, respectively, which are higher than any other solvents. The thermodynamic properties were also investigated, and the enthalpy change was the main driving force for CO capture.

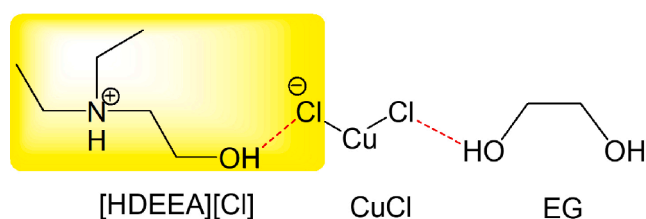
## 2. Experimental methods

### 2.1. Materials

2-Diethylaminoethanol hydrochloride ([HDEEA][Cl], 98%, CAS No. 14426–20-1) was purchased from Shanghai Macklin Biochemical Co., Ltd. Cuprous chloride (CuCl, 97%, CAS No. 7758–89-6) and ethylene glycol (EG, 99.5%, CAS No. 107–21-1) were obtained from Sinopharm Chemical Reagent Co., Ltd. CO (99.95%) and N<sub>2</sub> (99.9993%) were supplied from Hangzhou Jingong Gas Co., Ltd.

### 2.2. Preparation of the DESs

DESs used in this work were simply prepared through stirring mixtures of [HDEEA][Cl], CuCl and EG with different molar ratios (1:1:1, 1:1:2, and 1:1:4) under the protection of N<sub>2</sub> at 90 °C for 3 h. Before use, these DESs remove possible traces of water by freeze drying for 6 h. Water content of each DES was determined by Karl Fischer method (Mettler-Toledo DL32, Switzerland) and the value was less than 0.1%. Density (in g cm<sup>-3</sup>) and viscosity (in mPa s) from 293.2 to 343.2 K is



Scheme 1. Chemical structure of [HDEEA][Cl], CuCl and EG.

measured by the digital density meter Anton Paar DSA5000, and each measuring point was the automatic average of the repeated experiments for three times. FT-IR spectra were obtained on a VERTEX70 FT-IR spectrometer on a KBr disk. The DESs were then kept in a desiccator.  $M_{DES}$  is the molar weights of DES in g mol<sup>-1</sup>, and it could be calculated using Eq. (1): [50]

$$M_{DES} = n_{[HDEEA][Cl]} \times M_{[HDEEA][Cl]} + n_{CuCl} \times M_{CuCl} + n_{EG} \times M_{EG} \quad (1)$$

### 2.3. CO removal experiments

CO removal experiments by these DESs were performed using gas capture equipment which showed in Scheme 2. In this work, two chambers, one named gas storage chamber with volume  $V_1$  and another named equilibrium chamber with volume  $V_2$ , were put in the water bath with a desired temperature  $T$ . Then, a known amount of DES was put into the equilibrium chamber and vacuumed. Record the pressure in the equilibrium chamber as  $p_0$ , and then pass the CO from the gas cylinder into the gas storage chamber with a pressure of  $p_1$ . The CO is introduced into the equilibrium chamber from gas storage chamber through a needle valve. Then, locked the valve and record the pressure in the gas storage chamber as  $p'_1$ . The capture of CO is performed until the pressure remains constant for at least 1 h. It is considered that the gas–liquid equilibrium is reached, and the pressure of the equilibrium chamber is expressed as  $p_2$ . Thus, the CO partial pressure for the equilibrium capture capacity is  $p_e = p_2 - p_0$ . Therefore, the following Eq. (2) can be used to calculate the molar capacity  $C(p_e, T)$  of CO capture: [30]

$$C(p_e, T) = \rho_g(p_1, T)V_1 - \rho_g(p'_1, T)V_1 - \rho_g(p_e, T)(V_2 - w/\rho_{DES}) \quad (2)$$

where  $\rho_g(p_1, T)$ ,  $\rho_g(p'_1, T)$  and  $\rho_g(p_e, T)$  represent the CO density in mol cm<sup>-3</sup> under different  $p$  and  $T$  conditions;  $\rho_{DES}$  in g cm<sup>-3</sup> is the density of DES at  $T$ ;  $V_1$  and  $V_2$  in cm<sup>3</sup> respectively represent the volume of the two chambers, and  $w$  is the amount of DES in gram.

The CO capture experiment under higher pressure is to pass higher pressure CO into the gas storage chamber, and then introduce more CO into the equilibrium chamber to achieve a new balance. This work defines the capacity of CO as the molar ratio of CO to DESs. Duplicate experiments were run for DESs to obtain averaged values of CO capture. The average reproducibility of the capacity data in this work is 1%.

## 3. Results and discussion

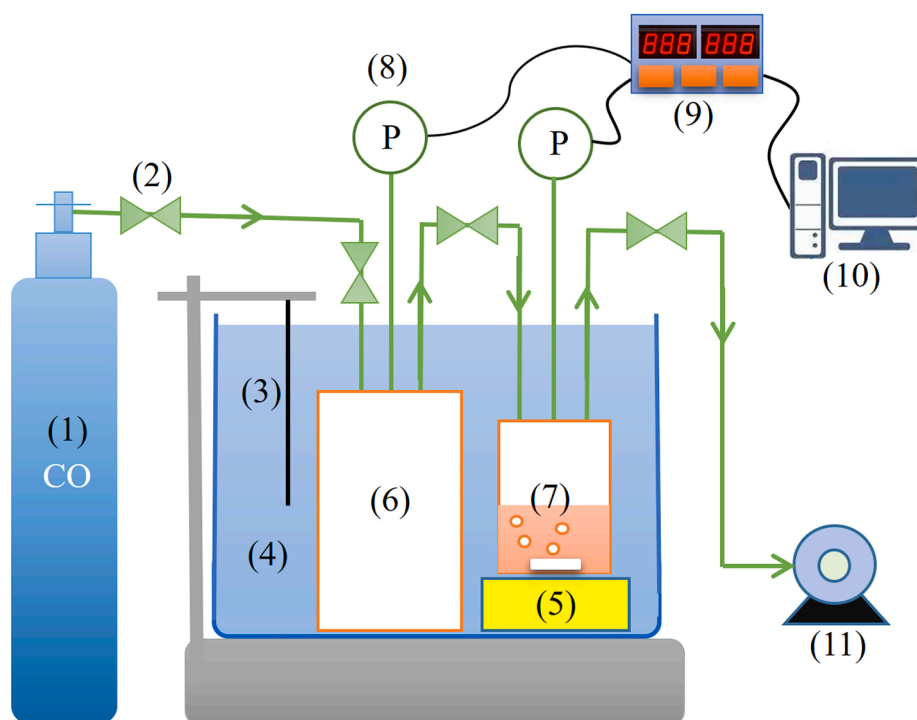
### 3.1. Physical properties.

Density and viscosity are important properties of DESs, especially for calculating the CO capacities by Eq. (2). Thus, the densities ( $\rho$ , in g cm<sup>-3</sup>) and viscosities ( $\eta$ , in mPa s) of three DESs [HDEEA][Cl] + CuCl + EG (1:1:1), [HDEEA][Cl] + CuCl + EG (1:1:2) and [HDEEA][Cl] + CuCl + EG (1:1:4) were measured at different temperatures ( $T$ , in K), and the results are shown in Fig. 1. These DESs have very low viscosity at room temperature. For example, the viscosities of [HDEEA][Cl] + CuCl + EG (1:1:1), [HDEEA][Cl] + CuCl + EG (1:1:2) and [HDEEA][Cl] + CuCl + EG (1:1:4) were 173.9, 65.1 and 40.4 mPa s at 293.2 K, respectively. It was found that the logarithm of density ( $\ln\rho$ ) decreased linearly as the temperature ( $T$ ) increased, while the logarithm of viscosity ( $\ln\eta$ ) increased linearly as the reciprocal of temperature ( $1/T$ ) increased. Clearly, the results indicated that the density and viscosity were decreased as the increase concentration of EG in DES. The following Equations (3) and (4) can be used to describe these relationships, respectively:

$$\ln\rho = a + bT \quad (3)$$

$$\ln\eta = \ln\eta_0 + \frac{E_\eta}{RT} \quad (4)$$

where  $a$  and  $b$  are fitting constants,  $\eta_0$  and  $E_\eta$  represent the pre-



**Scheme 2.** Experimental diagram of CO capture: (1) CO gas cylinder; (2) valve; (3) thermocouple; (4) thermostat water bath; (5) magnetic stirrer; (6) gas storage chamber; (7) equilibrium chamber with stirring bar; (8) pressure transducer; (9) numerical indicator; (10) personal computer; (11) vacuum pump.

exponential constant in mPa s and the flow activation energy of DES in  $\text{kJ mol}^{-1}$  while  $R$  is the universal gas constant of  $8.314 \text{ J mol}^{-1} \text{ K}^{-1}$ . The fitting values of  $a$ ,  $b$ ,  $\eta_0$  and  $E_\eta$  were listed in Table 1 while the fitting curves were shown in Fig. 1. It was found that Equations (3) and (4) could describe the temperature dependence of density and viscosity satisfactorily because of the high values of  $R^2$ . The values of  $E_\eta$  for [HDEEA][Cl] + CuCl + EG (1:1:1), [HDEEA][Cl] + CuCl + EG (1:1:2) and [HDEEA][Cl] + CuCl + EG (1:1:4) were calculated to be 39.11, 32.90 and  $30.13 \text{ kJ mol}^{-1}$ , respectively, indicating that the addition of EG is beneficial to CO capture.

### 3.2. CO capture measurement

The effect of CO partial pressure on CO capture capacities of these [HDEEA][Cl] + CuCl + EG DESs was investigated and the results are shown in Fig. 2. It was found that the CO capture capacities of [HDEEA][Cl] + CuCl + EG (1:1:1), [HDEEA][Cl] + CuCl + EG (1:1:2) and [HDEEA][Cl] + CuCl + EG (1:1:4) at 293.2 K and 1 bar were 0.140, 0.161 and 0.203 mol CO per mole DES, respectively. Thus, the order of CO capture capacity was [HDEEA][Cl] + CuCl + EG (1:1:1) < [HDEEA][Cl] + CuCl + EG (1:1:2) < [HDEEA][Cl] + CuCl + EG (1:1:4). These results indicated that the capacity increased with the increase concentration of EG in DESs [50]. It is known that the melting point of ternary DESs is lower than that of any component, and the viscosity of ternary DESs is lower than that of any other component, too. Thus, the activity of the DESs is released and increased through the addition of more EG. However, it is safely concluded that the main factor affecting CO solubility is the presence of copper(I) in these DESs [30,53]. On the other hand, the CO capture capacity was increased with the increase of CO partial pressure. For instance, CO capture capacity of [HDEEA][Cl] + CuCl + EG (1:1:4) at 293.2 K was rapid increased from 0.026 mol CO per mol DES under 0.1 bar to 0.203 and 0.564 mol CO per mol DES under 1 and 5 bar, respectively. It is also found that the absorption isotherm becomes flat under high CO partial pressure, similar to those found in CO chemisorption processes with  $[\text{C}_2\text{mim}]_x[\text{Cu}]_{1-x}[\text{SCN}]$  solutions described by Urriaga *et al.* [53] Based on the above results and related

reports, [30,53] the highly efficient CO capture by these DESs were mainly through the interaction between Cu(I) and CO.

We selected some typical DESs and ILs to compare the capture capacities of CO in mole CO per mole absorbent (Table 2). It can be seen that, [HDEEA][Cl] + CuCl + EG (1:1:4) DES showed the highest CO capture capacity among these active DESs and other solvents.

The effect of temperature on the CO capture capacity of [HDEEA][Cl] + CuCl + EG (1:1:4) DES at different CO partial pressure was investigated and the results are shown in Fig. 3. It was found that the CO capture capacity of [HDEEA][Cl] + CuCl + EG (1:1:4) significantly decreased with the increase of temperature. For example, the CO capture capacities of [HDEEA][Cl] + CuCl + EG (1:1:4) decreased from 0.203 to 0.057 mol CO per mole DES when the temperature increased from 293.2 to 323.2 K at 1 bar.

In order to study the effect of -OH group and EG in DESs on CO capture, the experiments of CO capture by [TEA][Cl] + CuCl and [HDEEA][Cl] + CuCl were designed for the comparison of CO capture by [HDEEA][Cl] + CuCl + EG (1:1:4), and the results are shown in Fig. 4. It was found that under the same capture conditions, (1) without EG, the CO capture capacities of [TEA][Cl] + CuCl and [HDEEA][Cl] + CuCl were lower than that of [HDEEA][Cl] + CuCl + EG (1:1:4), and (2) without EG and hydroxyl group, the CO capture capacities of [TEA][Cl] + CuCl were lower than that of [HDEEA][Cl] + CuCl and [HDEEA][Cl] + CuCl + EG (1:1:4). For instance, CO capture capacities of [HDEEA][Cl] + CuCl + EG (1:1:4), [HDEEA][Cl] + CuCl and [TEA][Cl] + CuCl were 0.080, 0.057, and 0.037 mol CO per mole DES at 313.2 K and 1 bar, indicating the -OH group and EG are good for CO capture. It is known that the melting point of ternary DESs is lower than that of any component, and the viscosity of ternary DESs is lower than that of any other component, too. Therefore, the activity of the DESs is released and increased through the addition of more EG.

Besides, CO absorption/desorption by [HDEEA][Cl] + CuCl + EG (1:1:4) as an example were also performed, and the results were showed in Fig. 5. It is shown that most of CO could be released by heating CO-saturated DES at 333.2 K under vacuum for 2 h. During these cycles, the capture capacity was well maintained indicating the good reusability

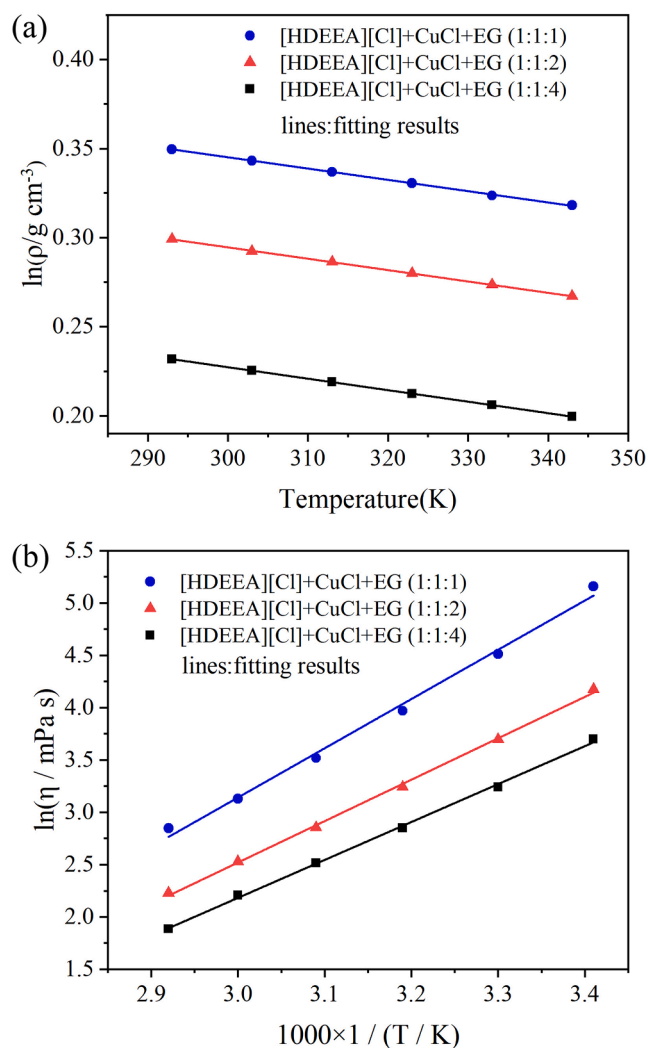


Fig. 1. Relationship between densities (a) or viscosities (b) of DESs with different temperatures.

of these DESs.

### 3.3. Mechanism of CO capture

To study the mechanism, [HDEEA][Cl] + CuCl + EG (1:1:4) DES as an example was characterized by ESI-MS, and the result is showed in Fig. 6a. It can be seen that there are two kinds of  $m/z$  peaks at 134.9 and 232.8 can be found, which are assigned to the anions  $[\text{CuCl}_2]^-$  and  $[\text{Cu}_2\text{Cl}_3]^-$ , respectively. These anions are responsible for the formation of complexes with CO and resulted in the efficient CO absorption into ionic solvents, according to the previous study by Tao *et al.* [52] Moreover, [HDEEA][Cl] + CuCl + EG (1:1:4), [HDEEA][Cl] + CuCl and [TEA][Cl] + CuCl before and after the absorption of CO at 293.2 K and 1 bar were characterized by FT-IR spectroscopy. It is shown that compared with the FT-IR spectrum of fresh [HDEEA][Cl] + CuCl + EG (1:1:4), [HDEEA][Cl] + CuCl and [TEA][Cl] + CuCl in Fig. 6b, new bands at

2088  $\text{cm}^{-1}$  were observed in the spectra of [HDEEA][Cl] + CuCl + EG (1:1:4), [HDEEA][Cl] + CuCl and [TEA][Cl] + CuCl after the capture of CO, indicating the interaction between CO and Cu(I) [30]. In addition, a new band at 1760  $\text{cm}^{-1}$  was observed in the spectrum of [HDEEA][Cl] + CuCl + CO while two new bands at 1774 and 1801  $\text{cm}^{-1}$  were observed in the spectrum of [HDEEA][Cl] + CuCl + EG (1:1:4) + CO, indicating the interaction of  $-\text{HO}\cdots\text{CO}$ . [56] Thus, the above results suggested that the presence of Cu(I) and  $-\text{OH}$  group in cuprous-based ternary DESs is good for CO capture, and Cu(I) plays a crucial role [53].

### 3.4. Thermodynamics analysis

According to experiment results and previous literatures, [30,53] capacity of CO by cuprous-based ternary [HDEEA][Cl] + CuCl + EG DESs is mainly owing to the interaction between Cu(I) and CO:



Thus, the equilibrium constant ( $K$ , dimensionless) of Eq. (5) under different temperature ( $T$ , in K) can be defined as Eq. (6):

$$K = \frac{C}{(1 - C) \times \frac{p_e}{p}} \quad (6)$$

where  $C$  (in  $\text{mol mol}^{-1}$ ) is the capacity under the CO partial pressure  $p_e$  (in bar). Therefore,

$$C = \frac{K \times \frac{p_e}{p}}{1 + K \times \frac{p_e}{p}} \quad (7)$$

The fitting curves for CO capture by these cuprous-based DESs at different temperatures and partial pressures are illustrated in Figs. 2 and 3, while the relationship between  $K$  and  $T$  can be It can be found in Fig. 7. It can be seen that a good linear relationship between  $\ln K$  and  $1/T$  was obtained with  $R^2$  of 0.96.

In order to understand the performance of CO capture by these DESs,

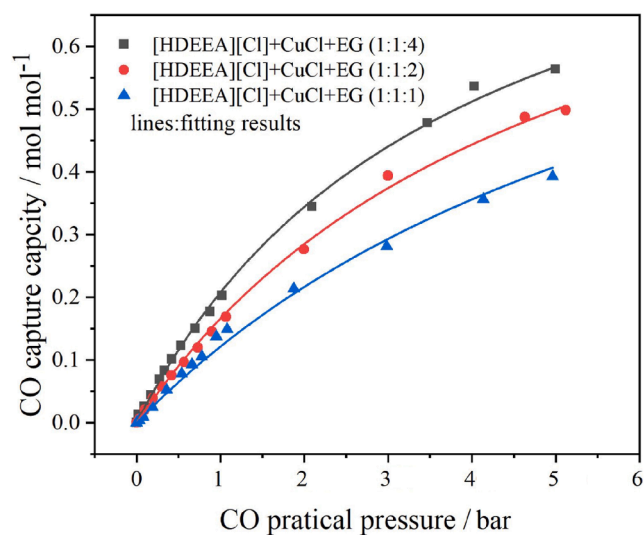


Fig. 2. CO capture capacity (in  $\text{mol CO mol}^{-1}$  DES) of three [HDEEA][Cl] + CuCl + EG DESs at 293.2 K and different CO partial pressures (in bar).

Table 1  
Fitting parameters for Equations (3) and (4).

| DES                             | Mw ( $\text{g mol}^{-1}$ ) | Parameters for Eq. (2) |                   |        | Parameters for Eq. (3) |          |       |
|---------------------------------|----------------------------|------------------------|-------------------|--------|------------------------|----------|-------|
|                                 |                            | $\alpha$               | $B [\times 10^4]$ | $R^2$  | $\eta_0 [\times 10^5]$ | $E_\eta$ | $R^2$ |
| [HDEEA][Cl] + CuCl + EG (1:1:4) | 500.7                      | 0.42                   | -6.44             | 0.9999 | 16.86                  | 30.13    | 0.999 |
| [HDEEA][Cl] + CuCl + EG (1:1:2) | 376.7                      | 0.49                   | -6.38             | 0.9999 | 8.69                   | 32.90    | 0.998 |
| [HDEEA][Cl] + CuCl + EG (1:1:1) | 314.7                      | 0.53                   | -6.34             | 0.9993 | 1.92                   | 39.11    | 0.994 |



**Table 2**

CO capture capacities (in mole CO per mole solvent) of typical DESs and other solvents.

| Solvent   | Temperature (K) | Capacity (mol mol <sup>-1</sup> ) |                        | Ref.      |
|---|-----------------|-----------------------------------|------------------------|-----------|
|   |                 | 0.1 bar                           | 1 bar                  |           |
| [HDEEA][Cl] + CuCl + EG (1:1:4)                       | 293.2           | 0.026                             | 0.203                  | This work |
| [HDEEA][Cl] + CuCl + EG (1:1:2)                       | 293.2           | 0.021                             | 0.161                  | This work |
| [HDEEA][Cl] + CuCl + EG (1:1:1)                       | 293.2           | 0.011                             | 0.140                  | This work |
| [BimH][Cl] + CuCl + ZnCl <sub>2</sub> (1:1:1)         | 353.2           | 0.006                             | 0.075                  | [52]      |
| [EimH][CuCl <sub>2</sub> ]                            | 293.2           | 0.012                             | 0.157                  | [30]      |
| [EimH][CuCl <sub>2</sub> ]                            | 303.2           | 0.011                             | 0.118                  | [30]      |
| [Emim][CuCl <sub>2</sub> ]                            | 303.2           | –                                 | 0.037                  | [30]      |
| [BimH][CuCl <sub>2</sub> ]                            | 303.2           | –                                 | 0.111                  | [30]      |
| [HimH][CuCl <sub>2</sub> ]                            | 303.2           | –                                 | 0.105                  | [30]      |
| [TEA][CuCl <sub>2</sub> ]                             | 303.2           | 0.008                             | 0.078                  | [29]      |
| [P <sub>4448</sub> ][Pen]                             | 298.2           | 0.027                             | 0.046                  | [27]      |
| [P <sub>4448</sub> ][Mho]                             | 298.2           | –                                 | 0.021                  | [27]      |
| [P <sub>4448</sub> ][Ido]                             | 298.2           | –                                 | 0.011                  | [27]      |
| [P <sub>4448</sub> ][Dib]                             | 298.2           | –                                 | 0.020                  | [27]      |
| [Bmim][Tf <sub>2</sub> N] <sup>a</sup>                | 303.2           | 1.5 × 10 <sup>-4</sup>            | 1.5 × 10 <sup>-3</sup> | [54]      |
| [Bmim][CH <sub>3</sub> SO <sub>4</sub> ] <sup>a</sup> | 293.2           | 2.6 × 10 <sup>-5</sup>            | 2.6 × 10 <sup>-4</sup> | [55]      |
| [Hmim][Cl]/CuCl                                       | 303.2           | 1.4 × 10 <sup>-3</sup>            | 0.014                  | [28]      |
| [Bmim][BF <sub>4</sub> ] <sup>a</sup>                 | 295.2           | 3.0 × 10 <sup>-5</sup>            | 3.0 × 10 <sup>-4</sup> | [26]      |
| [Bmim][PF <sub>6</sub> ] <sup>a</sup>                 | 295.2           | 3.1 × 10 <sup>-5</sup>            | 3.1 × 10 <sup>-4</sup> | [26]      |
| [Bmim][SbF <sub>6</sub> ] <sup>a</sup>                | 295.2           | 5.0 × 10 <sup>-5</sup>            | 5.0 × 10 <sup>-4</sup> | [26]      |
| [Bmim][CF <sub>3</sub> COO] <sup>a</sup>              | 295.2           | 5.2 × 10 <sup>-5</sup>            | 5.2 × 10 <sup>-4</sup> | [26]      |
| [Bmim][Tf <sub>2</sub> N] <sup>a</sup>                | 295.2           | 1.1 × 10 <sup>-4</sup>            | 1.1 × 10 <sup>-3</sup> | [26]      |
| Methanol  | 295.2           | 4.4 × 10 <sup>-5</sup>            | 4.4 × 10 <sup>-4</sup> | [26]      |
| Toluene   | 295.2           | 7.8 × 10 <sup>-5</sup>            | 7.8 × 10 <sup>-4</sup> | [26]      |
| 1-Hexene  | 295.2           | 2.1 × 10 <sup>-4</sup>            | 2.1 × 10 <sup>-3</sup> | [26]      |
| 1-Octene  | 295.2           | 1.7 × 10 <sup>-4</sup>            | 1.7 × 10 <sup>-3</sup> | [26]      |
| 1-Decene  | 295.2           | 1.3 × 10 <sup>-4</sup>            | 1.3 × 10 <sup>-3</sup> | [26]      |

<sup>a</sup> The solubilities at 1 bar were estimated according to Henry's law:  $K_H = P_{CO} / x_{CO}$ .

thermodynamic properties such as enthalpy change ( $\Delta H$ , in kJ mol<sup>-1</sup>), Gibbs free energy change ( $\Delta G$ , in kJ mol<sup>-1</sup>) and entropy change ( $\Delta S$ , in J mol<sup>-1</sup> K<sup>-1</sup>) were calculated according to Equations (8), (9), and (10), respectively, as following.

$$\frac{d \ln K}{d(1/T)} = -\frac{\Delta H}{R} \quad (8)$$

$$\Delta G = -RT \ln K \quad (9)$$

$$\Delta S = \frac{\Delta H - \Delta G}{T} \quad (10)$$

Thus, the value of  $\Delta H$  for [HDEEA][Cl] + CuCl + EG (1:1:4) was  $-39.63$  kJ mol<sup>-1</sup>, and the values of  $\Delta G$  and  $\Delta S$  were  $3.26$  kJ mol<sup>-1</sup> and  $-146.3$  J mol<sup>-1</sup> K<sup>-1</sup> at 293.2 K, respectively. The results of  $\Delta G$ ,  $\Delta H$ , and  $\Delta S$  at different temperatures were presented in Table 3. Owing to the values of  $\Delta G$ ,  $\Delta H$ , and  $\Delta S$  are all negative and  $|\Delta H| > T\Delta S$ , it can be safely concluded that the sign of  $\Delta G$  is determined by that of  $\Delta H$ , indicating that the enthalpy term is predominant for the favorable capture of CO

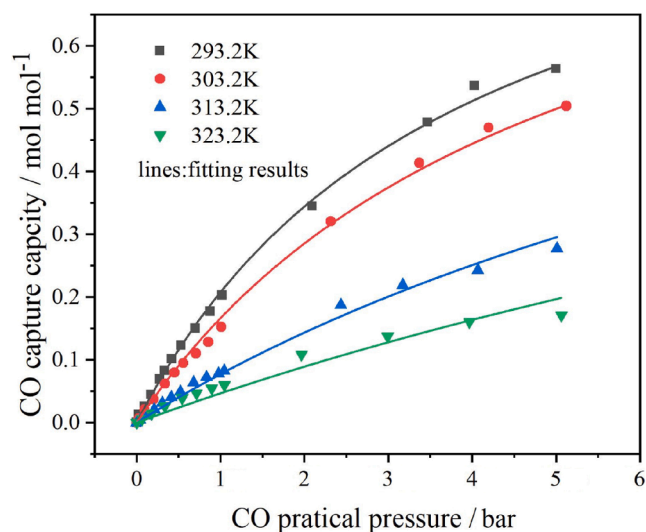


**Fig. 3.** CO capture capacities (in mol CO mol<sup>-1</sup> DES) of [HDEEA][Cl] + CuCl + EG (1:1:4) at different temperatures (in K) and different CO partial pressures (in bar).

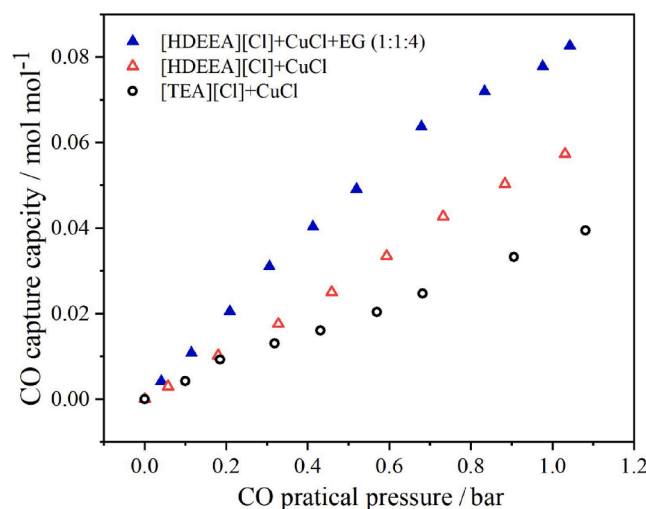


**Fig. 4.** Comparison of CO capture by [HDEEA][Cl] + CuCl + EG (1:1:4), [HDEEA][Cl] + CuCl and [TEA][Cl] + CuCl at 313.2 K and different partial pressures.

#### 4. Conclusions

Summarily, a series of active cuprous-based ternary DESs of [HDEEA][Cl] + CuCl + EG with different molar ratios such as 1:1:1, 1:1:2 and 1:1:4 were designed and prepared for highly efficient CO removal. The physical properties such as densities and viscosities of each DES were measured under different temperatures, and two equations were used to describe the relationship between these physical properties and temperature. The CO capture capacities of these DESs were measured under different CO partial pressures and different temperatures, and the capacity increased as partial pressure increased or temperature decreased. Besides, [TEA][CuCl<sub>2</sub>] and [HDEEA][CuCl<sub>2</sub>] were prepared to investigate the effect of  $-OH$  group on CO capture. FT-IR spectra were used for mechanism study. The results suggested that the presence of Cu(I) is crucial for efficient capture of CO by these ternary DESs while  $-OH$  groups and EG could release the activity of Cu(I). Thermodynamic properties of CO capture were also studied, and the enthalpy change was found to be the main driving force for CO capture by [HDEEA][Cl] + CuCl + EG (1:1:4). It is believed that CO capture by

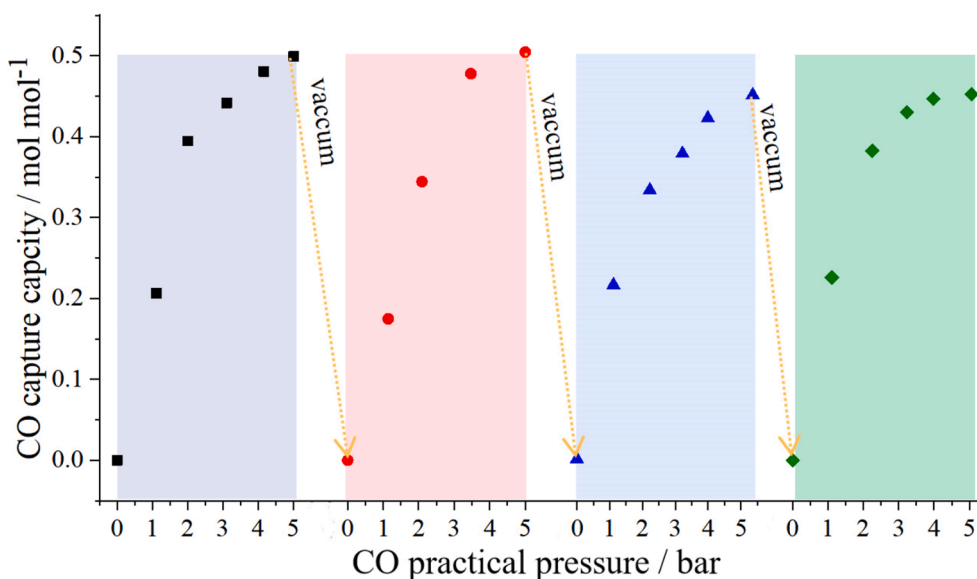


**Fig. 5.** 4 cycles of CO absorption/desorption by [HDEEA][Cl] + CuCl + EG (1:1:4) DES. CO absorption was carried out at 293.2 K, and desorption was carried out at 333.2 K and vacuum for 2 h.

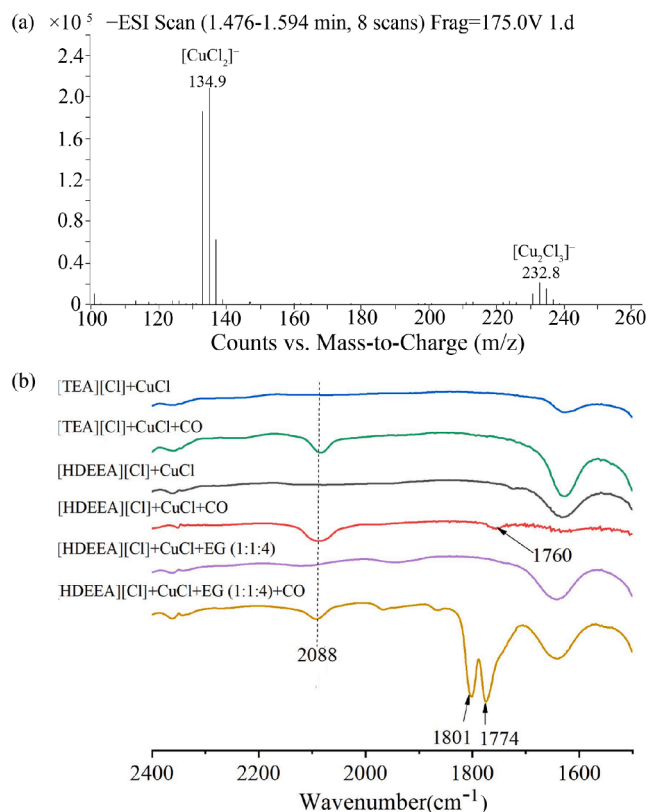


**Fig. 6.** (a) ESI-MS analysis for anion species of DES [HDEEA][Cl] + CuCl + EG (1:1:4). (b) FT-IR spectra of [TEA][CuCl<sub>2</sub>], [HDEEA][CuCl<sub>2</sub>] and [HDEEA][Cl] + CuCl + EG (1:1:4) before and after CO capture.

DESs provides an alternative way for efficient CO removal.

#### CRediT authorship contribution statement

**Guokai Cui:** Supervision, Conceptualization, Project administration, Funding acquisition, Writing - original draft, Writing - review & editing. **Kang Jiang:** Investigation, Validation, Data curation. **Huayan Liu:**

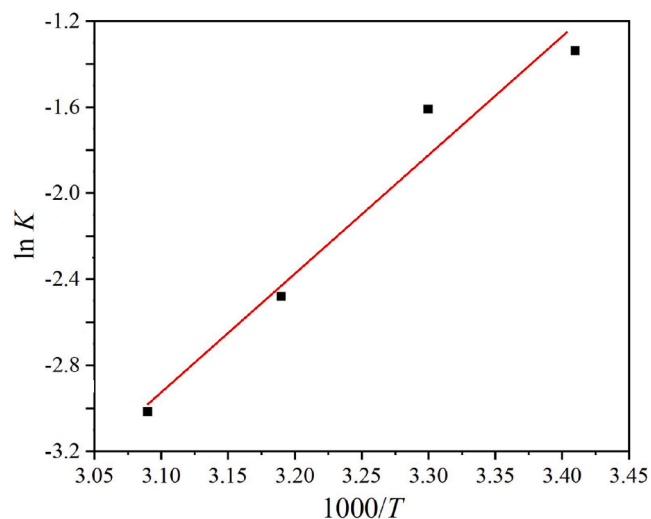


**Fig. 7.** linear fit of  $\ln K$  and  $1/T$  for CO absorption in [HDEEA][Cl] + CuCl + EG(1:1:4).

**Table 3**

$\Delta G$ ,  $\Delta H$ , and  $\Delta S$  of CO capture by [HDEEA][Cl] + CuCl + EG (1:1:4).

| Function                                     | T / K  |        |        |        |
|--|--------|--------|--------|--------|
|  | 293.2  | 303.2  | 313.2  | 323.2  |
| $\Delta G / \text{kJ mol}^{-1}$              | 3.26   | 4.06   | 6.46   | 8.11   |
| $\Delta H / \text{kJ mol}^{-1}$              | -39.63 |        |        |        |
| $\Delta S / \text{J mol}^{-1} \text{K}^{-1}$ | -146.3 | -144.1 | -147.2 | -147.7 |

Resources, Project administration, Data curation. **Zekai Zhang:** Resources, Project administration, Data curation. **Ying Zhou:** Formal analysis, Methodology, Visualization. **Ruina Zhang:** Formal analysis, Methodology, Visualization. **Hanfeng Lu:** Supervision, Project administration, Funding acquisition.

#### Declaration of Competing Interest

The authors declare that they have no known competing financial

interests or personal relationships that could have appeared to influence the work reported in this paper.

## Acknowledgement

This work was supported by the Natural Science Foundation of China (No. 22078294) and Zhejiang Provincial Natural Science Foundation of China (No. LZ21E80001 and LGF20E080018).

## References

- [1] L. Wang, Y. Zhou, Y. Yang, A. Subramanian, K. Kisslinger, X. Zuo, Y.-C. Chuang, Y. Yin, C.-Y. Nam, M.H. Rafailovich, Suppression of Carbon Monoxide Poisoning in Proton Exchange Membrane Fuel Cells via Gold Nanoparticle/Titania Ultrathin Film Heterogeneous Catalysts, *ACS Applied Energy Materials* 2 (5) (2019) 3479–3487.
- [2] P. Rejmak, M. Sierka, J. Sauer, Theoretical studies of Cu(I) sites in faujasite and their interaction with carbon monoxide, *Phys. Chem. Chem. Phys.* 9 (40) (2007) 5446–5456.
- [3] M.J. Battrum, W.J. Thomas, CARBON-MONOXIDE RECOVERY BY PRESSURE SWING ADSORPTION, *Chem. Eng. Res. Des.* 69 (2) (1991) 119–129.
- [4] G. Zarca, I. Ortiz, A. Urriaga, Copper(I)-containing supported ionic liquid membranes for carbon monoxide/nitrogen separation, *J. Membr. Sci.* 438 (2013) 38–45.
- [5] Á.A. Ramírez-Santos, C. Castel, E. Favre, A review of gas separation technologies within emission reduction programs in the iron and steel sector: Current application and development perspectives, *Sep. Purif. Technol.* 194 (2018) 425–442.
- [6] K. Huang, Y.-T. Wu, X.-B. Hu, Effect of alkalinity on absorption capacity and selectivity of SO<sub>2</sub> and H<sub>2</sub>S over CO<sub>2</sub>: Substituted benzoate-based ionic liquids as the study platform, *Chem. Eng. J.* 297 (2016) 265–276.
- [7] G. Cui, S. Lyu, F. Zhang, H. Wang, Z. Li, Y. Li, J. Wang, Tuning Ionic Liquids with Functional Anions for SO<sub>2</sub> Capture through Simultaneous Cooperation of N and O Chemical Active Sites with SO<sub>2</sub>, *Ind. Eng. Chem. Res.* 59 (49) (2020) 21522–21529.
- [8] J. Wang, Z. Song, H. Cheng, L. Chen, L. Deng, Z. Qi, Multilevel screening of ionic liquid absorbents for simultaneous removal of CO<sub>2</sub> and H<sub>2</sub>S from natural gas, *Sep. Purif. Technol.* 248 (2020), 117053.
- [9] G. Cui, J. Wang, S. Zhang, Active chemisorption sites in functionalized ionic liquids for carbon capture, *Chem. Soc. Rev.* 45 (15) (2016) 4307–4339.
- [10] X. Lv, K. Chen, G. Shi, W. Lin, H. Bai, H. Li, G. Tang, C. Wang, Design and tuning of ionic liquid-based HNO donor through intramolecular hydrogen bond for efficient inhibition of tumor growth, *Science, Advances* 6 (45) (2020) eabb7788.
- [11] C. Wang, G. Cui, X. Luo, Y. Xu, H. Li, S. Dai, Highly Efficient and Reversible SO<sub>2</sub> Capture by Tunable Azole-Based Ionic Liquids through Multiple-Site Chemical Absorption, *J. Am. Chem. Soc.* 133 (2011) 11916–11919.
- [12] G. Cui, J. Zheng, X. Luo, W. Lin, F. Ding, H. Li, C. Wang, Tuning Anion-Functionalized Ionic Liquids for Improved SO<sub>2</sub> Capture, *Angew. Chem., Int. Ed.* 52 (40) (2013) 10620–10624.
- [13] S. Zeng, H. Gao, X. Zhang, H. Dong, X. Zhang, S. Zhang, Efficient and reversible capture of SO<sub>2</sub> by pyridinium-based ionic liquids, *Chem. Eng. J.* 251 (2014) 248–256.
- [14] S. Ren, Y. Hou, K. Zhang, W. Wu, Ionic liquids: Functionalization and absorption of SO<sub>2</sub>, *Green Energy & Environment* 3 (3) (2018) 179–190.
- [15] F.-F. Chen, K. Huang, Y. Zhou, Z.-Q. Tian, X. Zhu, D.-J. Tao, D.-E. Jiang, S. Dai, Multi-Molar Absorption of CO<sub>2</sub> by the Activation of Carboxylate Groups in Amino Acid Ionic Liquids, *Angew. Chem., Int. Ed.* 55 (25) (2016) 7166–7170.
- [16] S. Zeng, X. Zhang, L. Bai, X. Zhang, H. Wang, J. Wang, D. Bao, M. Li, X. Liu, S. Zhang, Ionic-Liquid-Based CO<sub>2</sub> Capture Systems: Structure, Interaction and Process, *Chem. Rev.* 117 (14) (2017) 9625–9673.
- [17] Y. Huang, G. Cui, Y. Zhao, H. Wang, Z. Li, S. Dai, J. Wang, Preorganization and Cooperation for Highly Efficient and Reversible Capture of Low-Concentration CO<sub>2</sub> by Ionic Liquids, *Angew. Chem., Int. Ed.* 56 (43) (2017) 13293–13297.
- [18] X.-M. Zhang, K. Huang, S. Xia, Y.-L. Chen, Y.-T. Wu, X.-B. Hu, Low-viscosity fluorine-substituted phenolic ionic liquids with high performance for capture of CO<sub>2</sub>, *Chem. Eng. J.* 274 (2015) 30–38.
- [19] M. Taheri, R. Zhu, G. Yu, Z. Lei, Ionic liquid screening for CO<sub>2</sub> capture and H<sub>2</sub>S removal from gases: The syngas purification case, *Chem. Eng. Sci.* 230 (2021), 116199.
- [20] X. Zhang, W. Xiong, L. Peng, Y. Wu, X. Hu, Highly selective absorption separation of H<sub>2</sub>S and CO<sub>2</sub> from CH<sub>4</sub> by novel azole-based protic ionic liquids, *AIChE J.* 66 (6) (2020), e16936.
- [21] Y. Sun, S. Ren, Y. Hou, K. Zhang, Q. Zhang, W. Wu, Highly Reversible and Efficient Absorption of Low-Concentration NO by Amino-Acid-Based Ionic Liquids, *ACS Sustainable Chem. Eng.* 8 (8) (2020) 3283–3290.
- [22] K. Chen, G. Shi, X. Zhou, H. Li, C. Wang, Highly Efficient Nitric Oxide Capture by Azole-Based Ionic Liquids through Multiple-Site Absorption, *Angew. Chem., Int. Ed.* 55 (46) (2016) 14364–14368.
- [23] R. Qiu, X. Luo, L. Yang, J. Li, X. Chen, C. Peng, J. Lin, Regulated Threshold Pressure of Reversibly Sigmoidal NH<sub>3</sub> Absorption Isotherm with Ionic Liquids, *ACS Sustainable Chem. Eng.* 8 (3) (2020) 1637–1643.
- [24] P. Li, D. Shang, W. Tu, S. Zeng, Y. Nie, L. Bai, H. Dong, X. Zhang, NH<sub>3</sub> absorption performance and reversible absorption mechanisms of protic ionic liquids with six-membered N-heterocyclic cations, *Sep. Purif. Technol.* 248 (2020), 117087.
- [25] S. Zeng, L. Liu, D. Shang, J. Feng, H. Dong, Q. Xu, X. Zhang, S. Zhang, Efficient and reversible absorption of ammonia by cobalt ionic liquids through Lewis acid–base and cooperative hydrogen bond interactions, *Green Chem.* 20 (9) (2018) 2075–2083.
- [26] C.A. Ohlin, P.J. Dyson, G. Laurenczy, Carbon monoxide solubility in ionic liquids: determination, prediction and relevance to hydroformylation, *Chem. Commun.* 9 (2004) 1070–1071.
- [27] D.-J. Tao, F.-F. Chen, Z.-Q. Tian, K. Huang, S.M. Mahurin, D.-E. Jiang, S. Dai, Highly Efficient Carbon Monoxide Capture by Carbanion-Functionalized Ionic Liquids through C-Site Interactions, *Angew. Chem., Int. Ed.* 56 (24) (2017) 6843–6847.
- [28] O.C. David, G. Zarca, D. Gorri, A. Urriaga, I. Ortiz, On the improved absorption of carbon monoxide in the ionic liquid 1-hexyl-3-methylimidazolium chlorocuprate, *Sep. Purif. Technol.* 97 (2012) 65–72.
- [29] Z.-H. Tu, Y.-Y. Zhang, Y.-T. Wu, X.-B. Hu, Self-enhancement of CO reversible absorption accompanied by phase transition in protic chlorocuprate ionic liquids for effective CO separation from N<sub>2</sub>, *Chem. Commun.* 55 (23) (2019) 3390–3393.
- [30] Y.-M. Liu, Z. Tian, F. Qu, Y. Zhou, Y. Liu, D.-J. Tao, Tuning Ion-Pair Interaction in Cuprous-Based Protic Ionic Liquids for Significantly Improved CO Capture, *ACS Sustainable Chem. Eng.* 7 (13) (2019) 11894–11900.
- [31] G. Zarca, I. Ortiz, A. Urriaga, Recovery of carbon monoxide from flue gases by reactive absorption in ionic liquid imidazolium chlorocuprate(I): Mass transfer coefficients, *Chin. J. Chem. Eng.* 23 (5) (2015) 769–774.
- [32] F. Liu, Z. Xue, X. Lan, Z. Liu, T. Mu, CO<sub>2</sub> switchable deep eutectic solvents for reversible emulsion phase separation, *Chem. Commun.* 57 (5) (2021) 627–630.
- [33] X. Yang, Y. Zhang, F. Liu, P. Chen, T. Zhao, Y. Wu, Deep eutectic solvents consisting of EmimCl and amides: Highly efficient SO<sub>2</sub> absorption and conversion, *Sep. Purif. Technol.* 250 (2020), 117273.
- [34] Y. Sun, M. Gao, S. Ren, Q. Zhang, Y. Hou, W. Wu, Highly Efficient Absorption of NO by Amine-Based Functional Deep Eutectic Solvents, *Energy Fuels* 34 (1) (2020) 690–697.
- [35] B. Wang, J. Cheng, D. Wang, X. Li, Q. Meng, Z. Zhang, J. An, X. Liu, M. Li, Study on the Desulfurization and Regeneration Performance of Functional Deep Eutectic Solvents, *ACS Omega* 5 (25) (2020) 15353–15361.
- [36] H. Qin, X. Hu, J. Wang, H. Cheng, L. Chen, Z. Qi, Overview of acidic deep eutectic solvents on synthesis, properties and applications, *Green Energy & Environment* 5 (1) (2020) 8–21.
- [37] A.P. Abbott, D. Boothby, G. Capper, D.L. Davies, R.K. Rasheed, Deep Eutectic Solvents Formed between Choline Chloride and Carboxylic Acids: Versatile Alternatives to Ionic Liquids, *J. Am. Chem. Soc.* 126 (29) (2004) 9142–9147.
- [38] Y. Chen, X. Han, Z. Liu, D. Yu, W. Guo, T. Mu, Capture of Toxic Gases by Deep Eutectic Solvents, *ACS Sustainable Chem. Eng.* 8 (14) (2020) 5410–5430.
- [39] G. Cui, J. Liu, S. Lyu, H. Wang, Z. Li, R. Zhang, J. Wang, SO<sub>2</sub> absorption in highly efficient chemical solvent AChBr + Gly compared with physical solvent ChBr + Gly, *J. Mol. Liq.* 330 (2021), 115650.
- [40] L.L. Sze, S. Pandey, S. Ravula, S. Pandey, H. Zhao, G.A. Baker, S.N. Baker, Ternary Deep Eutectic Solvents Tasked for Carbon Dioxide Capture, *ACS Sustainable Chem. Eng.* 2 (9) (2014) 2117–2123.
- [41] G. Cui, M. Lv, D. Yang, Efficient CO<sub>2</sub> absorption by azolide-based deep eutectic solvents, *Chem. Commun.* 55 (10) (2019) 1426–1429.
- [42] J. Dou, Y. Zhao, H. Li, J. Wang, A. Tahmasebi, J. Yu, Mechanistic Study on the Removal of NO<sub>2</sub> from Flue Gas Using Novel Ethylene Glycol-tetrabutylammonium Bromide Deep Eutectic Solvents, *ACS Omega* 5 (48) (2020) 31220–31226.
- [43] J. Dou, Y. Zhao, F. Yin, H. Li, J. Yu, Mechanistic Study of Selective Absorption of NO in Flue Gas Using EG-TBAB Deep Eutectic Solvents, *Environ. Sci. Technol.* 53 (2) (2019) 1031–1038.
- [44] Y. Li, M.C. Ali, Q. Yang, Z. Zhang, Z. Bao, B. Su, H. Xing, Q. Ren, Hybrid Deep Eutectic Solvents with Flexible Hydrogen-Bonded Supramolecular Networks for Highly Efficient Uptake of NH<sub>3</sub>, *ChemSusChem* 10 (17) (2017) 3368–3377.
- [45] W.-J. Jiang, J.-B. Zhang, Y.-T. Zou, H.-L. Peng, K. Huang, Manufacturing Acidities of Hydrogen-Bond Donors in Deep Eutectic Solvents for Effective and Reversible NH<sub>3</sub> Capture, *ACS Sustainable Chem. Eng.* 8 (35) (2020) 13408–13417.
- [46] D. Deng, X. Deng, X. Duan, L. Gong, Protic guanidine isothiocyanate plus acetamide deep eutectic solvents with low viscosity for efficient NH<sub>3</sub> capture and NH<sub>3</sub>/CO<sub>2</sub> separation, *J. Mol. Liq.* 114719 (2020).
- [47] D. Yang, M. Hou, H. Ning, J. Zhang, J. Ma, G. Yang, B. Han, Efficient SO<sub>2</sub> absorption by renewable choline chloride–glycerol deep eutectic solvents, *Green Chem.* 15 (8) (2013) 2261–2265.
- [48] F. Liu, W. Chen, J. Mi, J.-Y. Zhang, X. Kan, F.-Y. Zhong, K. Huang, A.-M. Zheng, L. Jiang, Thermodynamic and molecular insights into the absorption of H<sub>2</sub>S, CO<sub>2</sub>, and CH<sub>4</sub> in choline chloride plus urea mixtures, *AIChE J.* 65 (5) (2019), e16574.
- [49] T.J. Trivedi, J.H. Lee, H.J. Lee, Y.K. Jeong, J.W. Choi, Deep eutectic solvents as attractive media for CO<sub>2</sub> capture, *Green Chem.* 18 (9) (2016) 2834–2842.
- [50] G. Cui, J. Liu, S. Lyu, H. Wang, Z. Li, J. Wang, Efficient and Reversible SO<sub>2</sub> Absorption by Environmentally Friendly Task-Specific Deep Eutectic Solvents of PPZBr + Gly, *ACS Sustainable Chem. Eng.* 7 (16) (2019) 14236–14246.
- [51] D. Deng, B. Gao, C. Zhang, X. Duan, Y. Cui, J. Ning, Investigation of protic NH<sub>4</sub>SCN-based deep eutectic solvents as highly efficient and reversible NH<sub>3</sub> absorbents, *Chem. Eng. J.* 358 (2019) 936–943.
- [52] D.-J. Tao, F. Qu, Z.-M. Li, Y. Zhou, Promoted absorption of CO at high temperature by cuprous-based ternary deep eutectic solvents, *AIChE J.* 67 (2) (2021), e17106.

- [53] G. Zarca, I. Ortiz, A. Urriaga, Novel solvents based on thiocyanate ionic liquids doped with copper(I) with enhanced equilibrium selectivity for carbon monoxide separation from light gases, *Sep. Purif. Technol.* 196 (2018) 47–56.
- [54] Q. Gan, Y. Zou, D. Rooney, P. Nancarrow, J. Thompson, L. Liang, M. Lewis, Theoretical and experimental correlations of gas dissolution, diffusion, and thermodynamic properties in determination of gas permeability and selectivity in supported ionic liquid membranes, *Adv. Colloid Interface Sci.* 164 (1) (2011) 45–55.
- [55] J. Kumelan, Á. Pérez-Salado Kamps, D. Tuma, G. Maurer, Solubility of the single gases H<sub>2</sub> and CO in the ionic liquid [bmim][CH<sub>3</sub>SO<sub>4</sub>], *Fluid Phase Equilib.* 260 (1) (2007) 3–8.
- [56] D.E. Milligan, M.E. Jacox, Infrared Spectrum and Structure of Intermediates in the Reaction of OH with CO, *J. Chem. Phys.* 54 (3) (1971) 927–942.